On-off Intermittency in locally coupled maps

Woosok Moon

November 2, 2010

Abstract

On-off intermittency refers to the special pattern of time series which experience long time periods of calm behavior followed by short periods at bursting. In particular, the Ricker Map, which is a model of the discrete evolution of the expected population of one species at a given generation, is implemented to generate on-off intermittency. The on-off intermittency generated by the Ricker Map also exhibits the main characteristics found in other dynamical systems. On-off intermittency in a locally connected Ricker Map is the main focus here. The signal transfer between adjacent maps changes the stability condition compared with that of a single map, which leads to different conditions for on-off intermittency in locally coupled Ricker maps. The evolution and signal transfer in locally connected maps is carefully studied using a simple continuous model which contains similar structure and generates on-off intermittency. Through this analysis, it is found that a specific map in a locally connected structure recieves positively correlated signals from the adjacent maps, which generates more on-stages compared with a single map which has the same parameters.

1 Introduction

A signal representing on-off intermittency exhibits two different states. One is an 'off' states, where the variable remain almost constant. The other is an 'on' state which is a short time period of sudden bursting in the time series. This on-off intermittency has attracted wide interest due to the potential that many phenomena are related to on-off intermittency. Examples include the solar cycle showing long time periods of calm interrupted by short bursting(Platt et al. 1993*a*), and earthquake occurrence(Bottiglieri & Godano 2007).

Suppose that there is a k-dimensional invariant manifold in an n-dimensional dynamical system, where $n > k$. The invariant manifold has a chaotic attractor whose stability can be controlled by a parameter, p. If p varies across a threshold, the distance between the trajectory and the invariant manifold remains very close to 0 for a long time and shows a sudden increase for a short duration. In this context, on-off intermittency can be defined(Platt et al. 1993*b*). This argument is discussed by considering the skew product structure in the dynamical system. Though the skew structure is not necessary for on-off intermittency, it facilitates the analysis of on-off intermittency. Let us consider the following

equations :

$$\dot{X} = F(X, \mu(t)), \tag{1}$$

$$\dot{Y} = G(Y, \nu_0), \text{ and} \tag{2}$$

$$\mu(t) = M(\mu_0, Y(t)), \tag{3}$$

wherein the parameter μ for the evolution of X is controlled by Y. In this system, if Y is responsible for the parameter μ traveling above and below a threshold with time, one could observe on-off intermittency in the time series for X. Consider an even simpler case of the logistic map for time evolution of X represented as $X_{t+1} = r_t X_t(1 - X_t)$. Here, r_t is the parameter determining the stability of the invariant manifold $X_t = 0$ and hence $r_t = A_0 + \sigma\xi_t$, where A_0 is the average of r_t and ξ_t is uniformly distributed noise between 0 and 1. Depending on the choice of A_0 and σ, we can generate an on-off intermittency signal in X(Toniolo et al. 2002).

This simple setting for on-off intermittency reveals several important characteristics of an on-off intermittency signal. Heagy et al. (1994) used uniformly distributed noise for driving a parameter to investigate the statistics of the duration of off-stages in on-off intermittency. They found that the probability density function ϕ of the duration of off-stages is proportional to $\phi^{-\frac{3}{2}}$, which is considered as the distinguishing characteristic of on-off intermittency relative to other non-intermittent signals or other intermittency signals. They also found numerically that the probability density function does not depend on the choice of the driving parameters, which hints of the possibility that the $-3/2$-law could be general for on-off intermittency generated by various dynamical structures. Toniolo et al. (2002) sought out various characteristics of on-off intermittency using power spectrum analysis and found a clear negative slope in a log-log scale plot. These results can be used to identify the on-off intermittency in the time series obtained from observation or experiments. For example, the time series of the earth quake occurence shows the $-3/2$-law in the probability density function of the duration of off-stages (Bottiglieri & Godano 2007). Even if we do not have an exact model for earthquake justifiably, we can speculate that the occurrence of earthquakes shows on-off intermittency.

This previous work opens the possibility that we can determine whether or not a signal observed exhibits on-off intermittency. However, the previous work used a single map to investigate the characteristics of on-off intermittency. It is not realistic that a single dynamical system is totally isolated from other nearby systems. For example, convection cells located in deep clouds can interact with neighboring cells, or the population of insects or fish at one location can be related to those at another location through migration or sharing of resources given by same environment. Considering the possible coupling with neighbors in realistic situations, it is worthwhile to investigate a simple form of interaction between dynamical systems under conditions for on-off intermittency.

In this report, we will use the Ricker Map, which is a generalized version of the logistic map for population dynamics. First, we will check whether the Ricker Map also contains on-off intermittency in trajectories that travel near an invariant manifold. We will also examine whether there is consistency in the characteristics of on-off intermittency that have been identified using different maps. Second, simple local coupling will be defined for the investigation of the role of the interaction. Based on the definition of local coupling, we will try to

find out how the signals in the local coupling structure evolve and transfer to adjacent maps. Numerical simulation and a possible theoretical approach will be provided.

2 Single Ricker Map

The Ricker Map (Ricker 1954) was first suggested by Bill Ricker to study the expected population of one specific species at a given generation. The Ricker Map is represented by a single discrete dynamical model in which the population at the generation $t+1$ is determined by the previous generation t with a prescribed growth rate and restriction given by environmental conditions like food, habitat and water. The Ricker Map is represented as

$$N_{t+1} = N_t e^{r(1-\frac{N_t}{K})}, \tag{4}$$

where N_t is the population at t and r is the growth rate. Th carrying capacity K represents the population size of the species that the environment can hold depending on resources like food or water. For simplicity in this study, K is assumed to be equal to be 1.0 and hence (4) becomes

$$N_{t+1} = N_t e^{r(1-N_t)} \tag{5}$$

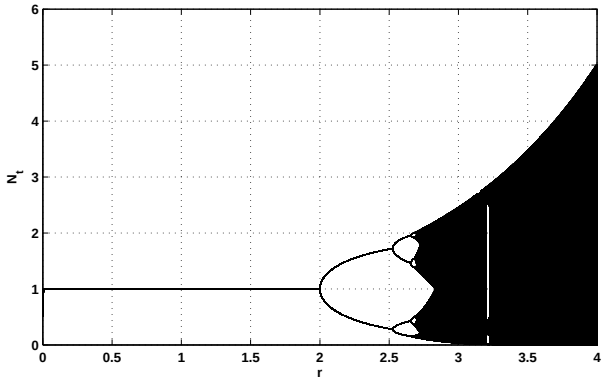

Figure 1: Bifurcation diagram for Ricker Map. If $r < 2.0$, N_t converges to 1.0. But if $r > 2.0$, N_t oscillates among several values, which demonstrates period-doubling bifurcation. At $r = 2.0$, one solution divides into two branches. Near $r = 2.5$, each solution bifurcates again and hence N_t travels around four values. As r increases, the periodic-doubling bifurcations continue and the number of solutions grows dramatically.

This discrete map shows different sequences of N_t depending on the value of r. If r is less than 2.0, N_t converges to 1.0. But if r is greater than 2.0, N_t starts to oscillate among several values. This situation is well displayed by a bifurcation diagram. Figure 1 shows the steady state solutions as a function of the value of r. When r is equal to 2.0, one solution divides into two branches which is called a period-doubling bifurcation. Then near $r = 2.5$, each solution

bifurcates again giving four solutions. As r increases further then, the period-doubling bifurcations continue and the number of solutions grows dramatically, which is shown in black in figure 1. Based on the bifurcation diagram, we can see that $N_t = 1.0$ is the invariant manifold whose stability is determined by r. If r is larger than 2.0, $N_t = 1.0$ becomes unstable. On-off intermittency can be generated when r moves across 2.0 in time. Under the assumption that r is independent of N_t (the skew product structure), we have to choose a way of determining r at each time step. Heagy et al. (1994) and Toniolo et al. (2002)'s works indicate that the method of determining r does not influence on-off intermittency. However, without specific physical constraints, we choose Gaussian white noise as our driving method with appeal to the central limit theorem. In realistic cases, r can be affected by various physical variables. The dimension of the dynamical system for r could be large. Therefore, many physical or environmental processes that evolve over a range of frequencies influence the time dependence of r. We can, therefore, think of the change of r in the context of Brownian motion as $r = r_0 + \sigma\xi$, where r_0 is the mean of r, ξ the Gaussian white noise whose mean and standard deviation are 0 and 1.0, respectively, and σ the intensity of noise. Hence the parameter r is controlled by two variables, r_0 and σ. We can ask if on-off intermittency is always seen in $|N_t - 1.0|$ in the parameter space, (r_0, σ), when r travels across 2.0.

Figure 2 shows time series with different r_0 and σ. For (a) and (c), we choose $r_0 = 2.1$, so that r_0 is in the parameter region where $N_t = 1.0$ is unstable. Then r is driven by Gaussian white noise whose amplitude is σ. In (a), σ is chosen to be 0.2, which does not produce an intermittent signal even though r moves through 2.0. The signal shown in figure 2(a) is similar to a noisy chaotic signal. When σ is increased to 0.4 in (c), the signal shows clear bursting after long calm period, which can be recognized as on-off intermittency. On-off intermittency is generated through a particular perturbation of r. Figure 2(b) shows an intermittent signal where $r = 7.0$ is chosen to be constant, but it is not on-off intermittency. On-off intermittency is generated when the perturbation of r changes the stability of the fixed point at each time step. The distinction between the intermittency shown in (b) and the on-off intermittency shown in (c) cannot be understood without information about r. We need further analyses to make a clear distinction.

According to figure 2, on-off intermittency emerges only for certain choices of r_0 and σ. Metta et al. (2010) suggested a method to find on-off intermittency by first computing the stability curve in a parameter space which consists of the mean value of the parameter and the intensity of the noise. They then used kurtosis to locate on-off intermittency in the parameter space. Larger values of kurtosis represent a signal that can be considered as on-off intermittency. We can follow the procedure here. First, we can think of the stability of N_t as a function of r_0 and σ. A necessary condition for on-off intermittency is that r_0 and σ must be chosen to lie inside the unstable region in the parameter space, (r_0, σ). Unless it is unstable, the time series converges to a fixed point so that the emergence of bursting is unlikely.

Consider the linearized equation near the fixed point, $N_t = 1.0$, for which we can let $N_t = \eta_t + 1$. After ignoring higher order terms, this gives

$$|\eta_{t+1}| = |1 - r_0 - \sigma\xi_t||\eta_t|. \tag{6}$$

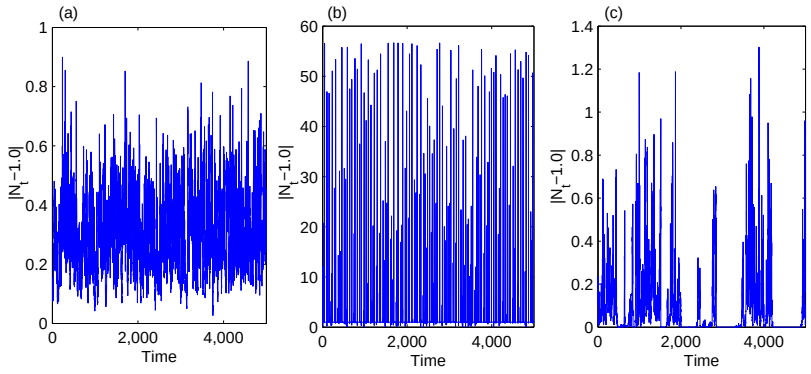

Figure 2: Sample time series of the driven variable N_t in the different r_0 and σ. (a) $r_0 = 2.1$, $\sigma = 0.2$; (b) $r_0 = 7.0$, $\sigma = 0.0$; (c) $r_0 = 2.1$, $\sigma = 0.4$. (a) shows noisy chaotic signal, which is non-intermittent signal. (b) is a kind of intermittent signal but not on-off intermittency. (c) shows an on-off intermittency.

From this relationship between N_{t+1} and N_t, we can determine $|\eta_t|$ as

$$|\eta_t| = \prod_{k=0}^{t-1} |1 - r_0 - \sigma\xi_k||\eta_0|. \tag{7}$$

Taking the logarithm of both sides, the equation becomes

$$\begin{aligned} \log|\eta_t| &= \sum_{k=1}^{t-1} \log|1 - r_0 - \sigma\xi_k| + \log|\eta_0| \\ &= t < \log|1 - r_0 - \sigma\xi_k| > + \log|\eta_0|. \end{aligned} \tag{8}$$

Here $< \cdot >$ represents the ensemble average and $< \log|1 - r_0 - \sigma\xi_k| >$ can be considered as the exponent of $|\eta_t|$. Therefore, the stability curve satisfies

$$< \log|1 - r_0 - \sigma\xi_k| > \; = 0. \tag{9}$$

The calculation of the ensemble average can be accomplished using the known probability density function for ξ_k.

$$< \log|1 - r_0 - \sigma\xi_k| >= \int_{-\infty}^{\infty} \rho(z)\log|1 - r_0 - \sigma z|dz, \tag{10}$$

where $\rho(z)$ is the normal distribution whose mean and standard deviation are 0.0 and 1.0, respectively.

Figure 3(a) shows the stability curve in (r_0, σ) parameter space, calculated using the equation (10). In the region bounded by the r_0 axis and the σ axis and the stability curve, all time series converge to the fixed point 1.0. Inside this region, it is impossible to find on-off intermittency. On-off intermittency

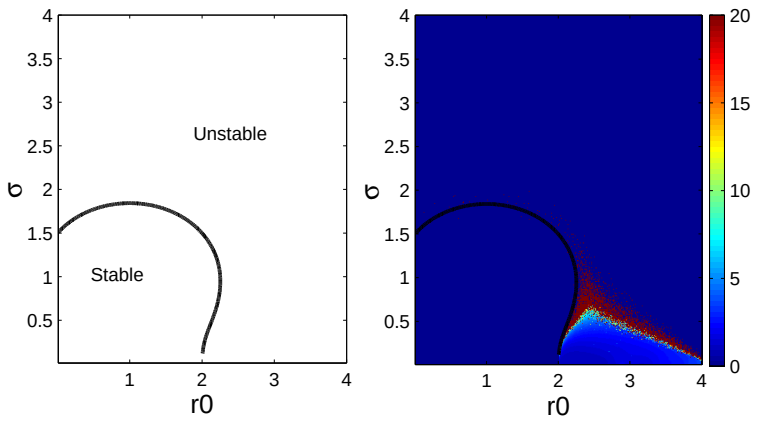

Figure 3: Stability curve and kurtosis at each r_0 and σ. (a) The stability curve is calculated using $< log|1 - r_0 - \sigma\xi_k| > = 0.0$. (b) At each r_0 and σ, kurtosis is calculated after generating the time series.

only exists outside of this region. To find the on-off intermittency outside of this stable region, kurtosis is a useful measure. Kurtosis is the statistical quantity used to detect infrequent extreme deviations. Higher kurtosis in this parameter space representative of on-off intermittency. In figure 3(b), we can see higher values of kurtosis in the area very close to stability curve. As suggested by previous research (Metta et al. 2010), there is on-off intermittency in the Ricker Map of the unstable region in parameter space and very near the stability curve.

In the Ricker Map, we have information about the parameters, r_0 and σ, which can lead to an on-off intermittency signal. Without information concerning r_0 and σ, however, we could be led by only looking at the signal itself. We need to seek other characteristics of on-off intermittency. First, we can examine the power spectrum of the time series generated by the Ricker Map. In figure 2, we used three time series including one on-off intermittency case. We can compare the power spectrum of these three cases. Figure 4 shows the power spectrum of the three cases shown in figure 2. Case (a) shows the power spectrum of the non-intermittency case which looks like a noisy chaotic time series. For lower frequencies, the slope is almost flat, which is analogous to white noise. We can see slope at higher frequencies. Case (b) has intermittency signals but not on-off intermittency. Instead of a slope, the power is intensified in higher frequencies. Case(c) shows on-off intermittency. Unlike the previous cases, a clear negative slope is shown from low frequencies to high frequencies. The slope shown in (c) can be considered as one of main features contained of on-off intermittency.

Another characteristic we have to consider is the duration of off-stages in

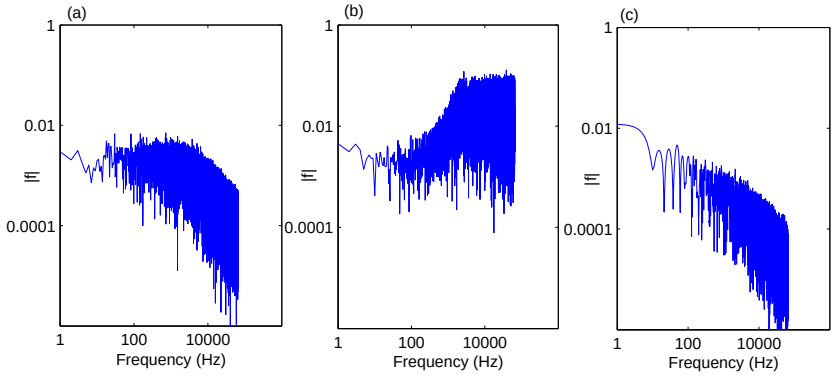

Figure 4: Power spectrum of three different cases. (a) $r_0 = 2.1$,$\sigma = 0.2$; (b) $r_0 = 7.0$,$\sigma = 0.0$; (c) $r_0 = 2.1$,$\sigma = 0.4$

the time series. The duration of an off stage is the time step between two consecutive on stages. The off stage can be defined in terms of the signal being below a certain value. Here, we will use 0.001 for the criterion for the off stage. Using the logistic map and a random process uniformly distributed between 0 and 1 for driving parameter, Heagy et al. (1994) proved that the probability density function (PDF) of T_ϕ (the duration of off-stages) is proportional to $T_\phi^{-\frac{3}{2}}$. They also showed numerically that the $-3/2$ law is maintained regardless of the details of the driving method. These could be another random process or any chaotic map. We can expect the same characteristics of on-off intermittency to occur in the Ricker Map. Figure 5 shows the probability density function of the duration of off-stages for three cases. The red line is the PDF for on-off intermittency, which is very close to a -3/2 slope line in log-log scale plot. The green line represents the PDF for the noisy chaotic case when $r_0 = 2.1$ and $\sigma = 0.2$. Here, the slope of the probability density function is quite different from -3/2. The last line is for another type of intermittency when $r_0 = 7.0$ and $\sigma = 0.0$, which is also distinct from on-off intermittency.

The $-3/2$ law can be used as a characteristic to determine whether a time series exhibits on-off intermittency. But it must be understood that this is not proven mathematically in general. To determine whether a given time series shows on-off intermittency, we have to use multiple analyses including power spectra and the PDF of the duration of off stages. Finally, if possible, we will try to construct a dynamical system for the time series and find the parameters necessary for the generation of on-off intermittency.

A single Ricker Map with Gaussian white noise generates on-off intermittency near the fixed point $N_t = 1.0$. The power spectrum and probability density function of the duration of off-stages of the Ricker Map are consistent with the results at several previous studies. The consistencies shown in on-off intermittency of the Ricker Map make it possible for us to use the Ricker Map for further analysis of on-off intermittency. As noted in the introduction, one

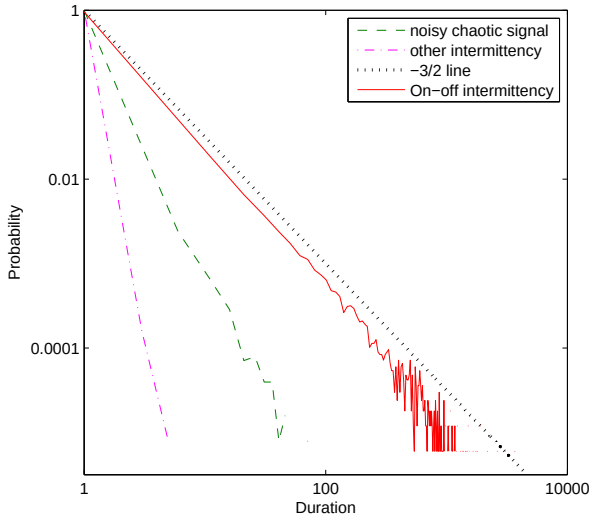

Figure 5: Probability density function of the duration of off-stages in log-log scales. On-off intermittency case is compared with two other cases. One of them is noisy chaotic time weries with $r_0 = 2.1$ and $\sigma = 0.2$. The other is other intermittency case when $r_0 = 7.0$ and $\sigma = 0.0$.

particular system is not totally isolated from other similar systems. More specifically, a group of species whose population is governed by the Ricker Map can interact with other nearby groups of same species. The interaction can occur in various forms. One example is the migration from one group to nearby groups. Another example is sharing of environmental resources. Therefore, our next step is to examine how on-off intermittency changes through in a single map under the possible interactions with adjacent maps.

3 Locally Connected Ricker Maps

Now we examine the dynamics of connected maps. For example, one group of salmon can interact with other groups via migration and sharing food or resources. Depending on the system, the form of the interaction may be different. As a starting point, the interaction can be assumed to be linear and local, which implies that maps are diffusively coupled. In a Ricker Map, local coupling can be understood as the dynamics of a metapopulation composed of many different populations that share individuals between different sites.

Lets consider the case of K locally connected maps all of which have the same parameter values,

$$N_{t+1}^k = (1-\epsilon) f(N_t^k; r_t^k) + \frac{\epsilon}{2}[f(N_t^{k-1}; r_t^{k-1}) + f(N_t^{k+1}; r_t^{k+1})], \qquad (11)$$

where $k = 1, 2, ..., K$, and

$$f(N_t^k; r_t^k) = N_t^k exp[r_t^k (1 - N_t^k)] \qquad (12)$$

where $r_t^k = r_0 + \sigma W_t^k$, and W_t^k is Gaussian white noise whose mean and standard deviation are 0 and 1, respectively. Also W_t^k is δ-correlated in space and time so that $< W_t^k W_s^m > = \delta_{km}\delta_{ts}$. The coupling coefficient ϵ determines the intensity of the local coupling. We also assume periodic boundary conditions which means that the K^{th} map is coupled to the $(K-1)^{th}$ map and 1^{st} map. The periodic boundary conditions mimic an infinite array of population sites.

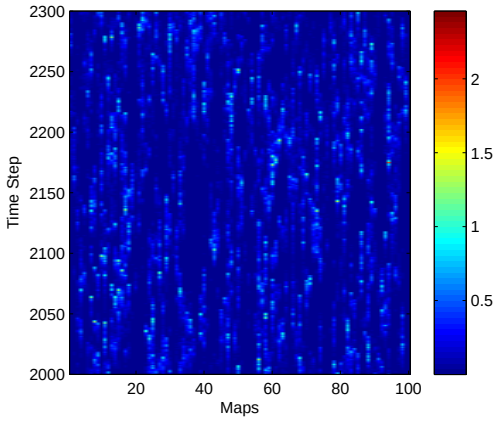

Figure 6: Signal pattern in a locally coupled map. $r_0 = 2; 1$, $\sigma = 0.4$, and $\epsilon = 0.01$ are used for the map.

Figure 6 shows an example of the local coupling of many maps, $r_0 = 2.1$, $\sigma = 0.4$, and $\epsilon = 0.01$. "On stages ", seen as bright color dots, appear from time to time after long period of "off stages ". The on-stages in one specific map seem to be related to that of the adjacent maps. Sometimes, the on-stage in one map seems to trigger in adjacent maps. We see a cluster of on-stages in the same space and time domain. This might be due to transfer between adjacent maps. Signal transfer can shape the on-off intermittency in the case of a local coupling.

A simple question is whether or not the local coupling is helpful in generating more on-stages. Figure 7 shows three examples of time series of one specific map among locally coupled maps. The coupling coefficient ϵ is different for the three examples. The first case has no coupling, the second has $\epsilon = 0.01$ and the third one has $\epsilon = 0.1$. According to the figure, the number of on stages generated during a fixed time increases as ϵ increases. Even though ϵ is quite small, the effect from this weak coupling is substantial. Figure 7 demonstrates that even a weak coupling can change the statistics of on-off stages dramatically.

In a single map, the most important issue is where on-off intermittency exists in the parameter space; it exists in the unstable region, but very close to the stability curve. Finding where on-off intermittency occurs in a parameter space must begin with the determination of the stability curve. For simplicity, we start with a 3-map local coupling. Even though only three maps are locally connected, we expect to find general characteristics of infinite coupled maps due to locality and periodic boundary conditions. Generally, finding the stability condition for a point in a parameter space is equivalent to finding the Lyapunov exponent. If the exponent is positive, it means the system is unstable. The stability curve

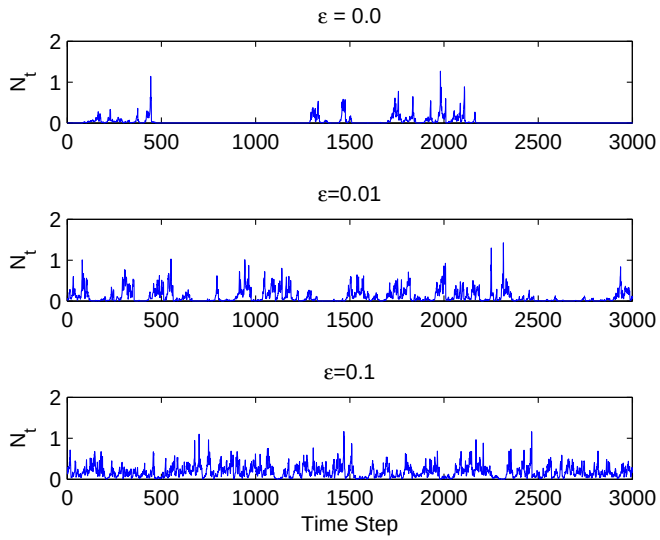

Figure 7: Time series of one specific map in locally coupled maps. Here, $r_0 = 2.1$ and $\sigma = 0.4$. The only difference among three examples is the magnitude of ϵ, the coupling coefficient.

is given by the set of the points where Lyapunov exponent is zero. To find the Lyapunov exponent, we have to linearize equation (8) near the fixed point $N_t = 1.0$. If $K = 3$, our linearized equation is

$$Z_{t+1} = Y_t Z_t, \tag{13}$$

where $Z_t = N_t - 1.0$ and

$$Y_t = \begin{bmatrix} (1-\epsilon)(1-r_0-\sigma\xi_1) & \frac{\epsilon}{2}(1-r_0-\sigma\xi_2) & \frac{\epsilon}{2}(1-r_0-\sigma\xi_3) \\ \frac{\epsilon}{2}(1-r_0-\sigma\xi_1) & (1-\epsilon)(1-r_0-\sigma\xi_2) & \frac{\epsilon}{2}(1-r_0-\sigma\xi_3) \\ \frac{\epsilon}{2}(1-r_0-\sigma\xi_1) & \frac{\epsilon}{2}(1-r_0-\sigma\xi_2) & (1-\epsilon)(1-r_0-\sigma\xi_3) \end{bmatrix}.$$

Therefore, Z_{t+1} is

$$Z_{t+1} = \left(\prod_{s=0}^{t} Y_s \right) Z_0. \tag{14}$$

Here, the Lyapunov exponent λ can be found using

$$\lambda = \lim_{t\to\infty} \frac{1}{t} \ln || \prod_{s=0}^{t} Y_s ||. \tag{15}$$

It is known that a limit for the calculation of λ exists even though the matrix is randomly determined at each time step. To determine the change of the Lyapunov exponent with local coupling, we fix $r_0 = 2.1$ and then vary σ and ϵ . Figure 8 shows the Lyapunov exponent in the parameter space (σ, ϵ) with fixed $r_0 = 2.1$. For a single map, with σ larger than 0.42, the Ricker Map

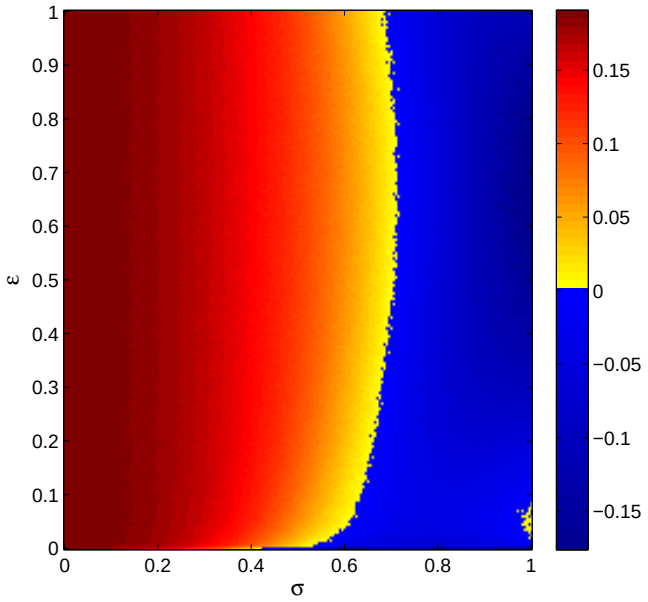

Figure 8: Lyapunov exponent in the parameter space (σ, ϵ) with fixed $r_0 = 2.1$.

becomes stable. In figure 8 we find $\sigma = 0.42$ when $\epsilon = 0.0$. Interestingly, a sudden change of stability with local coupling is formed for $0.42 < \sigma < 0.53$ where the stability condition suddenly changes with coupling. Even a weak coupling makes the system unstable. If σ is large enough, local coupling cannot change the stability. Lets consider a scenario relevant for this analysis. We think of the population of salmon governed by the Ricker Map. The growth rate r of one generation of salmon can be assumed to fluctuate due to a change in environmental resources at every time step. If the standard deviation of the fluctuation exceeds a certain threshold, for example $\sigma = 0.42$, the population of the salmon always maintains the fixed value even after many generations. Under the same environmental conditions, which implies that the mean and standard deviation of r are same, we can think of a case where salmon in a group start to migrate to nearby population groups. In this case, we expect a sudden sharp increase of the salmon population at some time step.

Figure 8 shows the increase of Lyapunov exponent with ϵ within some range of σ. If we remember that on-off intermittency is seen near the stability curve in the parameter space, we surmise that on-off intermittency formed in a single map could disappear with strong local coupling. First, we can check the power spectrum of the time series at each coupling coefficient. We know that a clear negative slope is found for on-off intermittency in the single map analysis. Figure 9 shows the power spectra for several values of ϵ. These power spectra are made by averaging the signals in 2^{13} maps after 2^{14} time steps. For the weak couplings, when ϵ is 0.1 or 0.2, the clear negative slope is shown in power spectrum. However, when $\epsilon = 0.5$ or $\epsilon = 0.8$, flatness over low frequencies appear, which also appeared in the noisy chaotic signal in the single map when

$r_0 = 2.1$ and $\sigma = 0.2$.

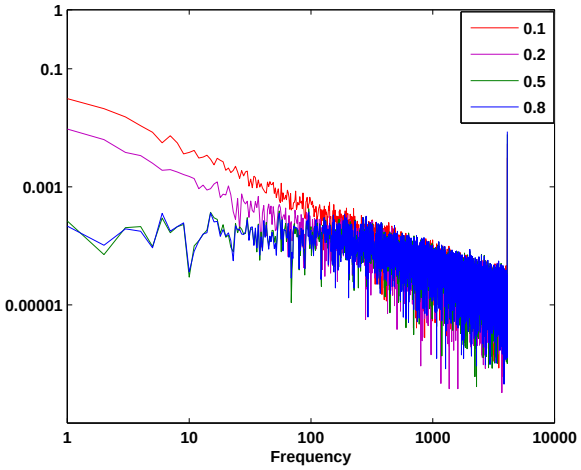

Figure 9: Power Spectra for several local couplings.

We have seen the change of stability and the statistics of on and off stages due to local coupling. This change could be made more evident if we trace how a certain on-stage is generated and how it interacts with other maps. For this job, we create 2^{13} maps locally coupled and run the system for 2^{14} time steps. A substantial number of on-stages can be sampled in the time and space domain. In this sampling, we also collect adjacent points centered on the on-stage in both the spatial and time domains. Figure 10 shows the average map over samples collected as described above. For this figure, we chose 20 adjacent maps and 40 time steps for sampling. The time step is from lag -20 to lag 20 centered on the on-stage. From this figure, we see how the signal in locally coupled maps evolves. Before the on-signal is generated, we see an increase of the signal of the map together with the adjacent maps. The on signal is not generated alone randomly. It can be correlated with adjacent maps so that the signals all increases together for the on-signals. This argument is refined further in the next section. After an on-signal is generated, the signal decays and, at the same time, diffuses away to adjacent maps. It is seen as a sharp V-shape, which may be related to the V-shape propagation of on-signals in the spatial and time domains from time to time.

The characteristics of on-off intermittency shown in this local coupling seems to be determined by how the signal is transfered and evolves with adjacent maps. We can conclude from numerical analysis that more on-signals are generated through the coupling. In a certain range of σ, the coupling even changes the stability of the map. This motivates a theoretical approach to explain how the signal of a specific map evolves with that of adjacent maps.

4 Signal Transferring in locally connected maps

Compared with a single Ricker Map, without rigorous quantification, we surmise that signals are coming to each map from adjacent maps, which may lead

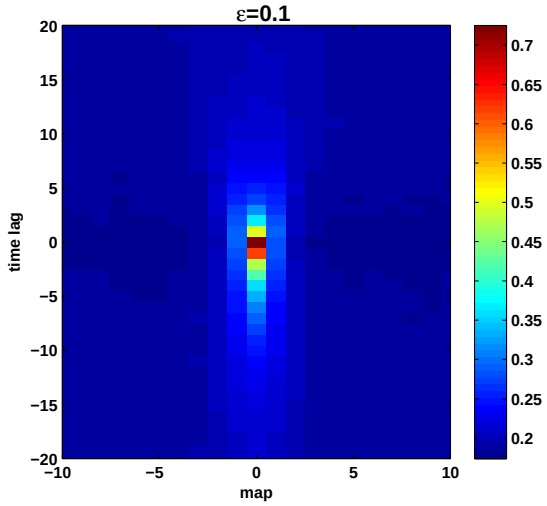

Figure 10: Average map over the area centered on on-stages in the spatial and time domains.

to more on stages in time series of locally coupled maps. However, without aid from numerical results, we can think of two different effects due to local coupling. As suggested above, more signals will come into each map from adjacent maps. Alternatively, the growing signal in each map could be diffused and transfered to adjacent maps, which could lengthen the duration of the off stage. Finding which one is more dominant or how to determine which case is preferred requires more precise analysis. However, these two possible effects only treat signal transferring. As we know, each map has its own system for increasing or decreasing signals, which might be a broader sort of reaction. Therefore, the combination of diffusion and reaction, which are randomly controlled, influences the signal pattern in the locally coupled maps.

On-off intermittency is characterized by long periods of calm stages and short periods of bursting. During a long period time of the off-stage, the signal, which is the distance from the fixed point, is negligibly small. Even though we can easily ignore the tiny signals during off-stages, the occurrence of the on-signal is completely governed by how the signal evolves during the off-stage, which implies that the generation of the on-stage is completely explained by the linearized equation near the fixed point or more generally the invariant manifold. The role of nonlinearity is to prevent further increase of the signal after the emergence of the on-signal and to make the signal return to the off stage. Heagy et al. (1994) proved the $-3/2$ law for the PDF of the duration of off stages using a linearized equation near the fixed point, which was possible due to the fact that the generation of the on-signal is governed by the signal growth during the off stage. Metta et al. (2010) explained the signal synchronization shown in two-map coupling based on the signal matching during the off stage. So, how the signal grows during the off period is the key process for explaining the statistics of the on-stages. Returning to the locally coupled maps, the main question is how signals grow and exchange information during off stages in

locally coupled maps. From this perspective, linearized equations near the fixed point during a particular off stage will be considered.

Despite the use of linearized equations, discrete maps are difficult to analyze analytically. A continuous model is more useful and can be constructed using stochastic calculus. Therefore, we use a time-continuous model qualitatively similar to the Ricker map to try to generate on-off intermittency. The model is a canonical cubic ODE,

$$\frac{dx}{dt} = \mu x - x^3, \tag{16}$$

whose stability near $x = 0$ is determined by the sign of μ; if μ is positive (negative), equation (16) is unstable (stable). The similarity to the Ricker map is seen as

$$\frac{dx}{dt} = -\frac{d}{dx}V = -\frac{d}{dx}(-\frac{1}{2}\mu x^2 + \frac{1}{4}x^4), \tag{17}$$

where the shape of V can tell us the stability of $x = 0$ and where stable solutions exist. Figure 11 shows the shape of V depending on the sign of μ near $x = 0$. When μ changes from negative to positive, the stable solution near $x = 0$ becomes unstable and two stable solutions near $x = \pm\sqrt{\mu}$ appear. This situation is analogous to a period-doubling bifurcation when r becomes slightly larger than 2 in the Ricker map. Therefore, if μ is perturbed near 0, on-off intermittency may be generated. Due to this qualitative similarity, we can use this continuous model to investigate on-off intermittency in locally connected maps.

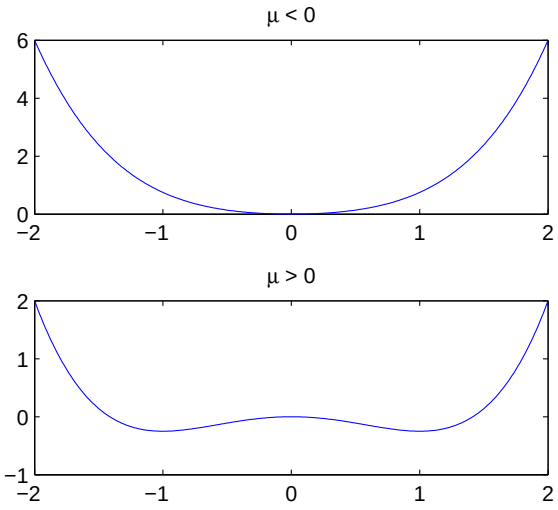

Figure 11: Shapes of V depending on the sign of μ

First, it is necessary to analyze on-off intermittency of the single map in this continuous model. Near $x = 0$, the linearized equation is

$$\frac{dx}{dt} = \mu x, \tag{18}$$

where μ is perturbed by some external process. Here, we simply choose Gaussian white noise to perturb μ as $\mu = \mu_0 + \sigma\xi$, where ξ and σ represent Gaussian white noise and intensity of the noise respectively. Moreover Gaussian white noise ξ can be written as time derivative of a Wiener process dW/dt. Equation (18) becomes and

$$dx = \mu_0 x dt + \sigma x dW. \tag{19}$$

Among other systems, this equation describes the evolution of option prices, where it is called the Black-Scholes model. Ito-calculus provides us with an exact solution, which is

$$x = \exp\left[(\mu_0 - \frac{1}{2}\sigma^2)t + \sigma W\right]. \tag{20}$$

We can determine the stability condition from the solution as

$$< (\mu_0 - \frac{1}{2}\sigma^2)t + \sigma W > = \ (\mu_0 - \frac{1}{2}\sigma^2)t \ > 0.$$

Therefore, the stability curve in the (μ_0, σ) domain is $\mu = \frac{1}{2}\sigma^2$. We expect on-off intermittency. Figure 12 shows a example of on-off intermittency near

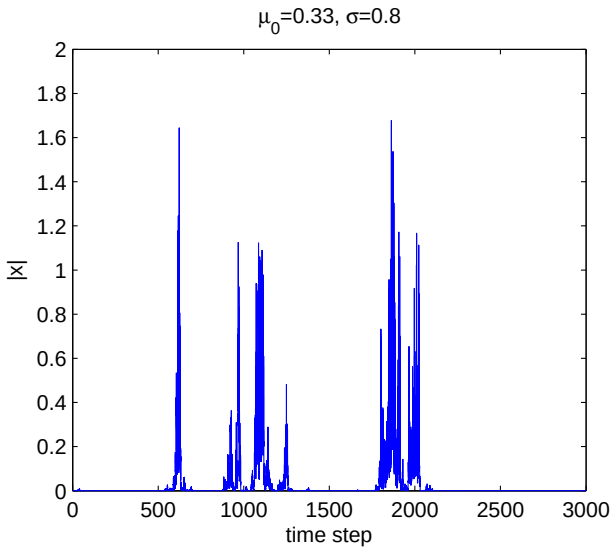

Figure 12: On-off intermittency when $\mu_0 = 0.33$ and $\sigma = 0.8$

stability curve in this continuous model.

We now construct the locally coupled maps. We focus on signal evolution and transfer during a certain off-stage so that the linearized equation near $x = 0$ will be considered in local coupling. Our equation is

$$\begin{aligned}\frac{dx_k}{dt} &= \mu_0 x_k + \sigma\xi_k x_K + \epsilon\mu_0\left(\frac{x_{k+1} + x_{k-1}}{2} - x_k\right) \\ &\quad + \epsilon\sigma\left(\frac{\xi_{k+1}x_{k+1} + \xi_{k-1}x_{k-1}}{2} - \xi_k x_k\right),\end{aligned} \tag{21}$$

where k and ϵ are the index of each map and the coupling coefficient, respectively. We can let $x_k = y_k e^{\mu_0 t}$ to remove the first term in the equation (21), thereby giving

$$\frac{dy_k}{dt} = \epsilon\mu_0 \left(\frac{y_{k+1} + y_{k-1}}{2} - y_k \right) + \sigma\xi_k x_k + \epsilon\sigma \left(\frac{\xi_{k+1} y_{k+1} + \xi_{k-1} y_{k-1}}{2} - \xi_k y_k \right), \tag{22}$$

which can be written in matrix form as

$$\frac{dY}{dt} = \epsilon\mu_0 AY + \sigma(I + \epsilon A)Y\xi, \tag{23}$$

where

$$A = \begin{pmatrix} -1 & \frac{1}{2} & 0 & 0 & \cdots & \frac{1}{2} \\ \frac{1}{2} & -1 & \frac{1}{2} & 0 & \cdots & 0 \\ 0 & \frac{1}{2} & -1 & \frac{1}{2} & \cdots & 0 \\ \vdots & & & & \ddots & \vdots \\ \frac{1}{2} & & \cdots & & \frac{1}{2} & -1 \end{pmatrix}$$

and

$$Y = (y_1, y_2, ..., y_n)^T,$$
$$Y\xi = (y_1\xi_1, y_2\xi_2, ..., y_n\xi_n)^T.$$

Here, A describes the structure of the periodic connection and is a symmetric matrix. We can easily construct the integral form of $Y(t)$, which is written as

$$Y(t) = \exp(\epsilon\mu_0 At)Y(0) + \sigma(I + \epsilon A) \int_0^t \exp(\epsilon\mu_0 A(t - t'))\, Y dW, \tag{24}$$

where

$$Y dW = (y_1 W_1, y_2 W_2, ..., y_n W_n),$$

and again W represents Wiener process. Because A is symmetric, it can be diagonalized and represented as $A = QDQ^T$ where D is the diagonal matrix whose diagonal terms are the eigenvalues of A. The above integral equation becomes

$$Y(t) = Q\exp(\epsilon\mu_0 Dt)Q^T Y(0) + \sigma Q(I + \epsilon D) \int_0^t \exp[\epsilon\mu_0 D(t - t')]\, Y dW \tag{25}$$

This integral form does not immediately give us any information. Even though we cannot expect a Gaussian distribution for the PDF of $Y(t)$, which means we have to know higher order moments, the correlation could give us some important information regarding the signal transfer between adjacent maps. From the above integral equation, we can construct the covariance matrix. Multiplying the transpose of $Y(t)$ and taking ensemble average, the covariance matrix can be represented as

$$< Y(t)Y(t)^T > = Q\exp(\epsilon\mu_0 Dt)Q^T < Y(0)Y^T(0) > Q\exp(\epsilon\mu_0 Dt)Q^T$$
$$+ \sigma^2 Q(I + \epsilon D) \int_0^t \int_0^t \exp(\epsilon\mu_0 D(t - t')Q^T < (Y dW)(Y dW)^T > \; Q\exp[\epsilon\mu_0 D(t - t')](I + \epsilon D)Q^T. \tag{26}$$

To simplify equation (26), we need information about the initial covariance structure. We seek the average behavior of signal transfer and hence it is reasonable to initially assume that each map is uncorrelated with any other map and the second moment of each map is identical. Mathematically, the assumption is

$$< y^2(0) >=< y_1^2(0) >=< y_2^2(0) >= ..... =< y_n^2(0) >$$
$$< y_i(0)y_j(0) >= 0, i \neq j$$

and dW represents a Wiener process which is independent at each time step and the noise input at each map is independent from other maps. Based on these facts and $dW \sim N(0, \sqrt{dt})$, we can deduce $< dW_i dW_j >= \delta_{ij} dt$. A more rigorous explanation is given by Ito-calculus as

$$\int_0^t \int_0^t f < (YdW)(YdW)^T > g = \int_0^t fgS,$$

where f and g are integrable functions and

$$S = \begin{pmatrix} < y_1^2 > dt & & & \\ & < y_2^2 > dt & & \\ & & \ddots & \\ & & & < y_n^2 > dt \end{pmatrix}.$$

There is no distinction between any of n maps because each map starts from the same condition. The statistical structure of all maps must be the same in time, which leads to

$$< y_1^2 >=< y_2^2 > = ... \ =< y_n^2 > .$$

Therefore, the integral equation for covariance can be simplified as

$$< Y(t)Y^T(t) > = Qexp(2\epsilon\mu_0 Dt)Q^T + \sigma^2 Q(I + \epsilon D) \int_0^t exp(2\epsilon\mu_0 Dt)(I + \epsilon D)Q^T < y^2 > \ dt'. \quad (27)$$

A technical difficulty exists for handling the $n \times n$ matrix in this equation. The simplest case is of 3 identical maps that are connected locally. Even in the 3-map case, we expect that the most important aspect for signal transference remains. For 3-map case we have

$$A = \begin{pmatrix} -1 & \frac{1}{2} & \frac{1}{2} \\ \frac{1}{2} & -1 & \frac{1}{2} \\ \frac{1}{2} & \frac{1}{2} & -1 \end{pmatrix},$$

$$Q = \begin{pmatrix} -\frac{1}{\sqrt{6}} & -\frac{1}{\sqrt{2}} & \frac{1}{\sqrt{3}} \\ \frac{2}{\sqrt{6}} & 0 & \frac{1}{\sqrt{3}} \\ -\frac{1}{\sqrt{6}} & \frac{1}{\sqrt{2}} & \frac{1}{\sqrt{3}} \end{pmatrix}, \text{ and } D = \begin{pmatrix} -\frac{3}{2} & 0 & 0 \\ 0 & -\frac{3}{2} & 0 \\ 0 & 0 & 0 \end{pmatrix},$$

If we insert Q and D into the integral equation, we find the integral equation for $< y^2 >$ as

$$< y^2 > = \left[\frac{1}{3} + \frac{2}{3}exp(-3\epsilon\mu_0 t)\right] < Y^2(0) > + \sigma^2 \int_0^t \left[\frac{1}{3} + \frac{2}{3}(1-\frac{3}{2}\epsilon)^2 exp(-3\epsilon\mu_0[t-t'])\right] < y^2 > dt'. \quad (28)$$

Differentiating with respect to t, we get

$$\frac{d}{dt} < y^2 >= -2\epsilon\mu_0 exp(-3\epsilon\mu_0 t) < y^2(0) > +\sigma^2(\frac{1}{3} + \frac{2}{3}(1-\frac{3}{2}\epsilon)^2) < y^2 > - 2\epsilon\mu_0\sigma^2(1-\frac{3}{2}\epsilon)^2 \int_0^t exp(-3\epsilon\mu_0(t-t')) < y^2(t') > dt', \quad (29)$$

and multiplying both sides by $\exp(3\epsilon\mu_0 t)$ and letting $q =< y^2 > \exp(3\epsilon\mu_0 t)$, we find

$$\frac{dq}{dt} - 3\epsilon\mu_0 q = -2\epsilon\mu_0 < y^2(0) > +\sigma^2 \left[\frac{1}{3} + \frac{2}{3}(1-\frac{3}{2}\epsilon)^2\right] q - 2\epsilon\mu_0\sigma^2(1-\frac{3}{2}\epsilon)^2 \int_0^t q dt'. \quad (30)$$

Differentiating again with respect to t on both sides, we get

$$\frac{d^2q}{dt^2} - (3\epsilon\mu_0 + \frac{1}{3}\sigma^2 + \frac{2}{3}\sigma^2(1-\frac{3}{2})^2)\frac{dq}{dt} + 2\epsilon\sigma^2\mu_0(1-\frac{3}{2}\epsilon)^2 q = 0. \quad (31)$$

The initial conditions are determined in the previous steps as

$$q(0) =< y^2(0) >, q'(0) = (\epsilon\mu_0 + \sigma^2 + \frac{2}{3}\sigma^2(1-\frac{3}{2}\epsilon)^2) < y^2(0) > .$$

A solution can be easily constructed for the second order differential equation with constant coefficients.

$$< y^2 >= C_1 e^{(\lambda_1 - 3\epsilon\mu_0)t} + C_2 e^{(\lambda_2 - 3\epsilon\mu_0)t}, \quad (32)$$

where

$$\lambda_{1,2} = \frac{1}{2}(3\epsilon\mu_0 + \frac{1}{3}\sigma^2 + \frac{2}{3}\sigma^2(1-\frac{3}{2}\epsilon)^2) \pm \sqrt{\frac{1}{4}(3\epsilon\mu_0 + \frac{1}{3}\sigma^2 + \frac{2}{3}(1-\frac{3}{2}\epsilon)^2)^2 - 2\epsilon\sigma^2\mu_0(1-\frac{3}{2}\epsilon)^2} \quad (33)$$

and

$$C_1 = \frac{< y^2(0) >}{\lambda_1 - \lambda_2}((\epsilon\mu_0 + \frac{1}{3}\sigma^2 + \frac{2}{3}\sigma^2(1-\frac{3}{2}\epsilon)^2) - \lambda_2),$$
$$C_2 = \frac{< y^2(0) >}{\lambda_1 - \lambda_2}(\lambda_1 - (\epsilon\mu_0 + \frac{1}{3}\sigma^2 + \frac{2}{3}\sigma^2(1-\frac{3}{2}\epsilon)^2)). \quad (34)$$

The coefficients, C_1 and C_2, are calculated from the two initial conditions. For $t \gg 0$, $< y^2 >$ is governed by $C_1 e^{(\lambda_1 - 3\epsilon\mu_0)t}$ and hence we can write

$$< y^2 > \sim C_1 e^{(\lambda_1 - 3\epsilon\mu_0)t}, \quad (35)$$

and we can compare this result with the single map. For the single map, the stochastic solution is $x(0)e^{(\mu_0-\frac{1}{2}\sigma^2)t+\sigma W}$. Because W follows $N(0,t)$, it is possible to find the $< x^2 >= x^2(0)e^{(\mu_0+\sigma^2)t}$. Figure 13 shows the comparison of $< y^2 >$ between the single map and the locally connected map. The x-axis represents the interaction coefficient ϵ and the y-axis is the difference of exponential exponent between the two cases. In this figure, $\lambda_1 - 3\epsilon\mu_0 - \sigma^2$ is negative for all interaction coefficients. The decrease of growth rate compared with that of the single map is caused by the local connection which suppresses the growth of the second moment of each map in the locally connected maps.

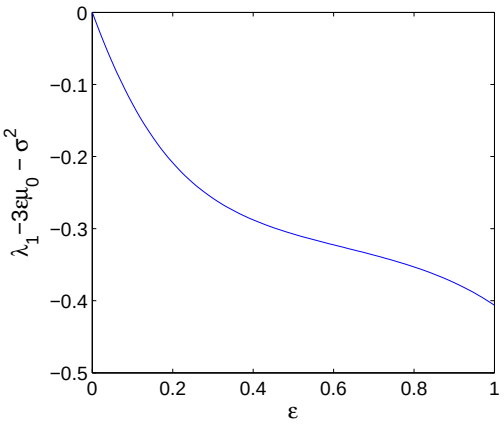

Figure 13: comparison of $< y^2 >$ between the single map and the locally connected maps

This result seems not to support the generation of more on stages in locally connected maps. A more revealing aspect may be the correlation between two adjacent maps. From the equation (12), we can find an equation for $< y_1 y_2 >$.

$$< y_1 y_2 > = (\frac{1}{3} - \frac{1}{3}e^{-3\epsilon\mu_0 t}) < y^2(0) > + \sigma^2 \int_0^t (\frac{1}{3} - \frac{1}{3}(1 - \frac{3}{2}\epsilon)^2 e^{-3\epsilon\mu_0(t-t')}) < y^2 > dt' \qquad (36)$$

In this equation $< y_1 y_2 >$ is determined by $< y^2 >$ which we calculated previously. Before finding the value of the integral, we discuss its structure. According to our previous calculation $< y^2 >$ is an exponentially increasing function with time. The correlation $< y_1 y_2 >$ is the time integral of $< y^2 >$. Therefore, we can expect that $< y_1 y_2 >$ increases exponentially with time. If we only care about the leading order form of the solution, we can approximate $< y_1 y_2 >$ as

$$< y_1 y_2 > \sim \frac{1}{3} C_1 \left[\frac{1}{\lambda_1 - 3\epsilon\mu_0} - \frac{(1 - \frac{3}{2}\epsilon)^2}{\lambda_1} \right] e^{(\lambda_1 - 3\epsilon\mu_0)t}. \qquad (37)$$

Obviously, the coefficients multiplying the exponential are positive. So, the correlation between two adjacent maps increases exponentially.

Returning to our linearized coupled equations, we can apply the above results to interpret each term in the equation (22). First, our underlying assumption

is that the system is unstable such that the signal, y_k, increases on average. Temporarily, y_k can experience a sudden or steady decrease but y_k eventually increases if we consider long time periods. We found from the above analysis that the y_k are positively correlated with the y_{k+1} and the y_{k-1}. In equation (22), the term $-\epsilon\mu_0 y_k$ decreases the growth rate of $< y_k^2 >$ compared with that of a single model. The term $\epsilon\mu_0(y_{k+1} + y_{k-1})/2$ has the most important role in this locally connected system due to the fact that y_{k+1} and y_{k-1} are positively correlated with y_k. If y_k starts to move away from the fixed point ($y_k = 0$), it provides positively correlated signals to y_k. More specifically, if y_k is negative, this term provides negative values for y_k at the next time step. If y_k is positive, the opposite sequence occurs. This term drives y_k away from the fixed point. When we consider other terms $(1 - \epsilon)\sigma\xi_k y_k + \epsilon\sigma(\xi_{k+1}y_{k+1} + \xi_{k-1}y_{k-1})/2$, we must recall that y_k, y_{k+1} and y_{k-1} are positively correlated, and ξ_{k+1}, ξ_k and ξ_{k-1} are independent Gaussian white noise terms. The sum of these noisy terms is negligible compared with the other terms. As a result, local connection sets up the condition for the positive correlation between adjacent systems, which provides the positively correlated signals to one specific map.

Our calculation in the context of a linearized local connection gives a picture of how the signals among adjacent maps evolve and transfer during a long time period of the off stage. Under unstable conditions, adjacent maps together have the tendency to escape from the fixed point. This process is rapidly accelerated due to the transfer of positively correlated signals from one specific map to adjacent maps. This mechanism can explain the generation of more on stages when we increase the coupling coefficient ϵ.

5 Conclusion

The Ricker Map which is represented as $N_{t+1} = N_t e^{r_t(1-N_t)}$ has a fixed point at $N_t = 1.0$. The fixed point is stable or unstable depending on the value of r_t relative to 2.0. If r_t is driven by Gaussian white noise near $r_t = 2.0$, on-off intermittency is generated. The on-off intermittency in the Ricker Map has characteristics consistent with those discussed in previous work. The power spectrum for on-off intermittency shows a clear slope in log-log scale plots. Most importantly, the probability density function ϕ for the duration of the off stages in the Ricker Map is also proportional to $\phi^{-3/2}$. This consistency leads us to a more realistic consideration of the Ricker Map.

The Ricker Map is used for the evolution of the population of one species at one generation. A realistic environment in this species is not isolated from other similar systems. Therefore, on-off intermittency in the Ricker Map is investigated under a locally connected situation. That mimics the possible interaction among neighboring species under the same environmental conditions. Even though the exact form of interaction is not shown, as a first step, we use a linear coupling with adjacent maps based on the coupling coefficient ϵ. The magnitude of ϵ represents the intensity of the interaction. According to numerical simulations, the statistics of on-off intermittency are changed relative to a single map that has the same parameters. Moreover, the stability condition changes due to local coupling. Within some range of σ, the locally connected Ricker maps become unstable even though the single map is stable under the same parameters. The mechanism for explaining the change caused by the lo-

cal coupling must be strongly related to the evolution and transfer of signals between adjacent maps.

Signal evolution and transfer of information in a locally coupled system was considered theoretically using a time-continuous model similar to the Ricker Map. This continuous model enables us to use stochastic calculus to make progress. We found that the signal in a specific map belonging to the locally coupled system is positively correlated with the signal in adjacent maps. The positively correlated signals that come from adjacent maps are added to the signal in the map for the next time step. Under unstable conditions, this feedback due to correlations with adjacent maps causes the signal to accelerate away from the fixed point, which explains the change of statistics of on-off intermittency under the local coupling.

6 Acknowledgments

I am grateful to Antonello Provenzale for initiating this project and his helpful advice. I am also thankful to Neil Balmforth. After discussion with him, I could realize that I was making mistakes in my calculation. Finally, I thank to all the GFD fellows for sharing great experience with me and especially to those who have spent long night with me in Walsh cottage during this summer.

References

Bottiglieri, M. & Godano, C. (2007), 'On-off intermittency in earthquake occurrence', *Phys. Rev. E* **75**(2), 026101.

Heagy, J. F., Platt, N. & Hammel, S. M. (1994), 'Characterization of on-off intermittency', *Physical Review E* **49**(2), 1140–1150.

Metta, S., Provenzale, A. & Spiegel, E. A. (2010), 'On-off intermittency and coherent bursting in stochastically-driven coupled maps', *Chaos, Solitons & Fractals* .

Platt, N., Spiegel, E. A. & Tresser, C. (1993*a*), 'The intermittent solar cycle', *Geophys. Astrophys. Fluid Dynamics* **73**, 147–161.

Platt, N., Spiegel, E. A. & Tresser, C. (1993*b*), 'On-off intermittency : A mechanism for bursting', *Physical Review Letters* **70**(3), 279–282.

Ricker, W. E. (1954), 'Stock and recruitment', *J. Fisheries Res. Board Can.* **11**, 559–623.

Toniolo, C., Provenzale, A. & Spiegel, E. A. (2002), 'Signature of on-off intermittency in measured signals', *Phys. Rev. E* **66**(6), 066209.